Colorimetric analysis of eye fundus structures with multispectral retinography

Francisco J. Burgos-Fernández [1,*], Tommaso Alterini [1], Fernando Díaz-Doutón [1], Meritxell Vilaseca [1]

[1] Centre for Sensors, Instruments and Systems Development, Universitat Politècnica de Catalunya, Rambla Sant Nebridi 10, 08222 Terrassa, Spain; francisco.javier.burgos@upc.edu, tommaso.alterini@upc.edu, fernando.diaz-douton@upc.edu, meritxell.vilaseca@upc.edu.

* Corresponding author: francisco.javier.burgos@upc.edu

Abstract

The analysis of the eye fundus is critical to prevent retinal and choroidal diseases since most of them cause no symptoms at early stages. Treating them when the very first signs appear is crucial to avoid vision losses. To this end, the color of eye fundus structures of healthy and diseased patients was assessed from images acquired with a novel multispectral fundus camera (400 nm – 1300 nm) with high spectral and spatial resolution. Characteristic color traits were found: in healthy eyes, large CIEDE2000 color differences were reported between arteries and veins due to different blood oxygenation; the contrast of nerve fibers/fovea was enhanced, giving rise to relevant color differences; in eyes with age related macular degeneration, lesions such as drusen could be better distinguished than with traditional color retinography; alterations of the optic disk in patients with glaucoma were also assessed, showing remarkable CIEDE2000 values when compared to healthy patients.

Keywords: *eye fundus, colorimetric analysis, multispectral imaging, spectral reflectance.*

INTRODUCTION

Retinography is one of the most frequently used techniques to evaluate the eye fundus when the presence of an alteration is suspected since it provides fast and comprehensive color information of retinal structures in a wide field of view. Depending on the pathology, different structures and substances are present and it is important for them to be clearly visualized, especially at early stages, to make a proper diagnosis. Some of the most frequent diseases affecting the eye fundus are age related macular degeneration (ARMD) and glaucoma.

ARMD often causes central vision loss, Coleman et al. (2008); a high concentration of lipofuscin, a yellow-brown lipid residual from phagocytosis of photoreceptors, may contribute to this. Lipofuscin leads to soft drusen, which can vary from pale white to bright yellow, have no defined boundaries and can be larger than 1000 µm; they are the first clinical sign of AMRD and are associated to a higher risk of vision loss. On the other hand, hard drusen have sharper edges than soft drusen, are smaller and less likely to progress to a greater atrophy, Abdelsalam et al. (1999). Glaucoma is a pathology associated with high intraocular pressure. It mainly affects the retinal nerve fiber layer (NFL) and can be diagnosed by observing the optic disk from fundus and/or optical coherence tomography images, Yanoff and Sassani (2015). As found in the literature, the degeneration of the NFL causes reflectance and color changes at the center and periphery of the optic disk that can be used for the early detection of this pathology, Huang et al. (2012).

The accurate spectral and colorimetric characterization of healthy fundus structures is also crucial when looking for possible alterations. The NFL is especially visible at short-intermediate visible wavelengths while the optic disc is clearly observable up to 1000 nm, mainly due to the myelin covering the nerve fibers, Yanoff and Sassani (2015). Retinal vessels are seen brighter for long visible wavelengths (>580nm) since they absorb the shorter ones and can be easily discriminated up to 800 nm because veins (deoxygenated blood) present higher light absorption than arteries (oxygenated

blood) in this range, Berendschot et al. (2003). Macular pigment acts as a blue filter with a maximum absorption at 460 nm, while those structures containing melanin - retinal pigmented epithelium (RPE) and choroid - also absorb intermediate visible wavelengths up to 600 nm, Bone et al. (2003).

All these spectral and colorimetric features of diseased and healthy fundus structures may go unnoticed by traditional fundus cameras since they show limitations related to metamerism caused by their intrinsic colorimetric nature, as they use RGB cameras with only three broadband channels in the visible range. Multispectral imaging offers a compromise solution between spectroscopic systems and RGB imaging, joining the strengths of these two approaches: the spectral sampling and the pixel-wise evaluation. In this context, the goal of this work is to study the colorimetric and spectral features of diseased and healthy eye fundus structures by means of a fast visible and infrared multispectral fundus camera (400 nm – 1300 nm) with high spectral and spatial resolution, Alterini et al. (2019).

MATERIALS AND METHODS

Subjects

This study was conducted on diseased and healthy subjects at the Institute of Ocular Microsurgery (Barcelona, Spain) and at the University Vision Center of the Universitat Politècnica de Catalunya (Terrassa, Spain). Table 1 provides some demographic data of the diseased and healthy patients. The inclusion criteria for the diseased patients were presenting any eye fundus pathology such as ARMD and glaucoma. Exclusion criteria were the diagnosis of any other ocular or systemic disease affecting the eye different from the previous ones, especially those that notably alter the transparency of the ocular media such as mature cataracts. Inclusion criteria for healthy patients were stricter: best-corrected visual acuity equal to or higher than 0.9 in decimal units, intraocular pressure equal to or lower than 21 mmHg, and no history of any ocular pathology or trauma. Additionally, all patients presented a subjective spherical refraction comprised between ± 15D and astigmatism ≤ 2D due to the operating range of the prototype. Ethical committee approval was obtained and all patients provided written informed consent before any examination. The Declaration of Helsinki tenets of 1975 (as revised in Tokyo in 2004) were followed throughout the study.

Condition	Eyes	Patients	Females (%)	Males (%)	Age (mean ± SD [range]; years)
Diseased	194	97	61.3	38.7	64.2 ± 17.1 [19, 95]
Healthy	126	81	54.4	45.6	47.9 ± 17.4 [19, 81]

Table 1: Number of eyes, patients, gender distribution and age for the diseased and healthy patients (SD = standard deviation).

Multispectral fundus camera

The multispectral fundus camera prototype consists of two detection arms, one from the visible to the near infrared (VIS-NIR: 400 - 950 nm) and another for the NIR range (960 - 1300 nm), Alterini et al. (2019). Three light emitting diode rings integrate the illumination system, covering 15 spectral bands with peak wavelengths of 416 nm, 450 nm, 471 nm, 494 nm, 524 nm, 595 nm, 598 nm, 624 nm, 660 nm, 732 nm, 865 nm, 955 nm, 1025 nm, 1096 nm, and 1213 nm. The system is non-mydriatic (no need for pupil dilation) with 30-degree angular field of view. As mentioned before, the prototype has a

spherical compensation range of ± 15D. Despite the large spectral range covered, the acquisition of the 15 images, one for each spectral band, only lasts 613 ms (220 ms for the VIS-NIR spectral bands and 393 ms for the NIR ones). Although it is above the acquisition time of traditional fundus cameras (≈250 ms), Carl Zeiss Meditec AG (2021) and Institute of Ocular Microsurgery (2021), which only takes one color image, it can be considered a fast acquisition, thus avoiding imaging problems caused by eye movements and blinking, while causing similar inconvenience to the patient as in traditional retinography.

Image processing and colorimetric analysis

Firstly, raw images were preprocessed to remove reflections and non-uniformities caused by the optics and the illumination source of the system. Afterwards, spectral reflectance values were retrieved from multispectral images when dividing them by a calibrated reference white (BN-R98-SQC, Gigahertz-Optik GmbH, Germany). CIELAB parameters were then computed using D65 illuminant for diseased and healthy eyes. Since the transmittance of the ocular media preceding the retina might slightly differ from one subject to another, CIEDE2000 color differences were computed between different fundus structures within each eye. This is a similar approach to that used by ophthalmologists, as they identify eye fundus structures for the chromatic and luminous differences with respect to the general appearance of the eye fundus.

RESULTS AND DISCUSSION

Beyond the study of chromatic coordinates, the high spectral sampling obtained with the multispectral fundus camera offered great discrimination among fundus structures, highlighting details that may remain hidden using traditional color fundus cameras.

Mean ± SD CIEDE2000 color differences between fundus structures were computed for all healthy patients evaluated. The different absorption properties of arteries and veins due to oxy- and deoxyhemoglobin were translated into 6.0 ± 3.0 CIEDE2000 units; the difference in absorption between both structures caused by different oxygen concentration in blood was especially noticeable around 600 nm (Figure 1 left). Nerve fibers are hardly observable in traditional RGB retinographies but using the multispectral prototype they are linked to 6.6 ± 4.6 CIEDE2000 units with respect to the fundus. Figure 1 center displays how the NFL is highlighted at short visible wavelengths as they are very superficial and short wavelengths are reflected superficially whereas longer ones penetrate deeper into the retinal tissue. Likewise, the fovea has no defined boundaries in color fundus images but, taking advantage of its blue filter behavior, the spectral evaluation performed with the multispectral camera led to 6.2 ± 3.9 CIEDE2000 units when compared to the fundus; this phenomenon was also observed at short visible wavelengths (Figure 1 right).

Some representative cases for specific diseases and structures are reported next: CIEDE2000 values of 3.5 units were obtained between hard and soft drusen for a patient with exudative ARMD (Figure 2 left). This color difference was mainly caused by the higher L* of hard drusen, which could be attributed to a decrease in melanin absorption since they are usually associated to cell loss in the RPE. In another eye, a degeneration of the RPE caused by a dry ARMD reported a CIEDE2000 value of 4.9 units when compared to the eye fundus (i.e., without structures). As shown in Figure 2 center, the most remarkable finding in this case was that the lesion could not be detected in the RGB image acquired with a traditional fundus camera due to metamerism, which proves the importance of the spectral sampling on the detection of subtle lesions and for the early diagnosis of retinal diseases.

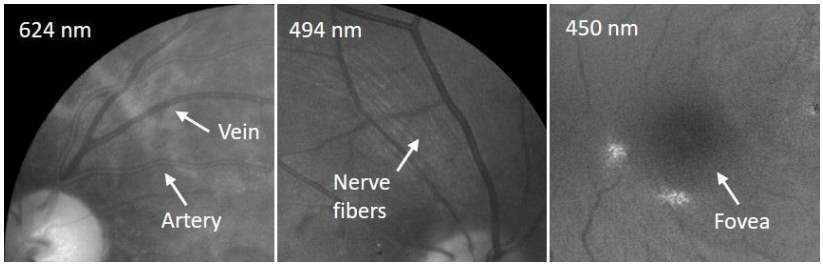

Figure 1: Zoomed spectral images at different wavelengths from healthy patients. Left: arteries and veins are clearly differentiable at 624 nm, being brighter the formers. Center: nerve fibers are highlighted at short visible wavelengths. Right: fovea appears darker at short visible wavelengths, being more distinguishable from the fundus.

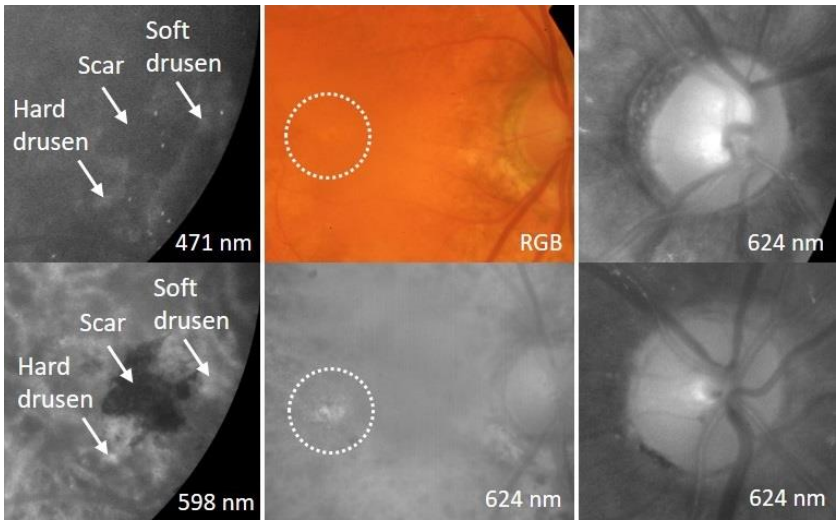

Figure 2: Zoomed spectral images at different wavelengths for eyes affected by exudative (left) and dry ARMD (center), glaucoma (right-top) and a healthy eye (right-bottom). Left: lesions are more distinguishable at longer visible wavelengths. Center: a subtle lesion is detected by the developed multispectral fundus camera while unnoticed when using traditional RGB retinography. Right: It can be observed how the reflectance is higher for the central part of the optic disc in the glaucomatous eye (top) than in the healthy one (bottom), also covering a larger area in the former.

An eye fundus affected by glaucoma was colorimetrically analyzed by comparing the center and periphery of the optic disk. A CIEDE2000 color difference of 13.9 units was found, being well above the mean CIEDE2000 values for healthy patients (9.5 ± 3.4 units). As it is summarized in Table 2, the higher color difference for the glaucomatous eye was mainly attributable to an increase of luminance in the central part of the optic disk (Figure 2 right-top). One hypothesis of this behavior may be that, as glaucoma causes a degeneration of optic disk layers, the lamina cribrosa and the myelinated fibers exiting the eye ball are more exposed taking to a higher reflectivity. Additionally, the eye with glaucoma presented a purer yellow appearance since a* was very close to 0, which corresponds to what has been found by other authors, Huang et al. (2012), who reported flatter spectra with a reduced contribution of short visible wavelengths in eyes suffering this disease.

Condition	Optic disk zone	L*	a*	b*	CIEDE2000
Glaucomatous eye	Periphery	76.0	3.5	5.2	13.9
	Center	91.6	0.5	16.3	
Healthy eyes	Periphery	72.6 ± 5.7	9.7 ± 7.3	12.0 ± 8.1	9.5 ± 3.4
	Center	83.6 ± 5.4	12.1 ± 6.9	17.9 ± 8.7	

Table 2: CIELab color coordinates and CIEDE2000 color differences for the center and periphery of the optic disk in the glaucomatous eye and in the healthy dataset.

CONCLUSIONS

The colorimetric and spectral analysis based on the images acquired by the multispectral fundus camera offers precise information and quantitative metrics than can improve the discrimination between healthy and diseased structures. The colorimetric data retrieved from the spectrally sampled reflectance curves allows a better differentiation between arteries and veins due to different blood oxygenation. The proposed evaluation might also contribute to a better detection of structures that are commonly difficult to see using color fundus images, such as the NFL and the fovea. When applied to fundus pathologies such as ARMD and glaucoma, diseased structures can be precisely located, even lesions that may remain hidden in traditional retinography. Future work will focus on increasing the dataset of diseased eyes.

ACKNOWLEDGEMENTS

This project has received funding from the European Union's Horizon 2020 research and innovation programme under Marie Skłodowska-Curie grant agreement No. 801342 (Tecniospring INDUSTRY) and the Government of Catalonia's Agency for Business Competitiveness (ACCIÓ). This research was also supported by the Ministerio de Economía, Industria y Competitividad (MINECO), the Agencia Estatal de Investigación (AEI) and the European Regional Development Fund (FEDER) under the grant DPI2017-89414-R.

DISCLAIMER

This work only expresses the opinion of the authors and neither the European Union nor ACCIÓ are liable for the use made of the information provided.

REFERENCES

Abdelsalam, A., L. Del Priore, and M. A. Zarbin. 1999. Drusen in age-related macular degeneration: pathogenesis, natural course, and laser photocoagulation-induced regression. *Survey of Ophthalmology* 44(1): 1–29.

Alterini, T., F. Díaz-Doutón, F. J. Burgos-Fernández, L. González, C. Mateo, M. Vilaseca. 2019. Fast visible and extended near-infrared multispectral fundus camera. *Journal of Biomedical Optics* 24(9): 096007-1–096007-7.

Berendschot, T. J. M., P. J. DeLintb, and D. V Norren. 2003. Fundus reflectance—historical and present ideas. *Progress in Retinal and Eye Research* 22(2): 171–200.

Bone, R. A., J. T. Landrum, L. H. Guerra, and C. A. Ruiz. 2003. Lutein and Zeaxanthin Dietary Supplements Raise Macular Pigment Density and Serum Concentrations of these Carotenoids in Humans. *The Journal of Nutrition* 133(4): 992–998.

Carl Zeiss Meditec AG (Jena, Germany). Accessed June 16, 2021. ZEISS CLARUS 500. https://www.zeiss.com/meditec/int/product-portfolio/retinal-cameras/clarus-500.html#specifications

Coleman, H. R., C.-C. Chan, F. L. 3rd Ferris, and E. Y. Chew. 2008. Age-related macular degeneration. *Lancet* 372(9652): 1835–1845.

Huang, X. R., Y. Zhou, R. W. Knighton, W. Kong, and W. J. Feuer. 2012. Wavelength-dependent change of retinal nerve fiber layer reflectance in glaucomatous retinas. *Investigative Ophthalmology & Visual Science* 53(9): 5869–5876.

Institute of Ocular Microsurgery (Barcelona, Spain). Accessed June 16, 2021. Retinography. https://www.imo.es/en/pruebas-diagnosticas/retinography

Yanoff, M., and J. W. Sassani. 2015. *Optic Nerve* in Ocular Pathology (7th ed.). London: W.B. Saunders.